HHS Public Access

Author manuscript

Mol Pharm. Author manuscript; available in PMC 2016 April 12.

Published in final edited form as:

Mol Pharm. 2015 April 6; 12(4): 1289–1298. doi:10.1021/mp500847s.

Codelivery of Small Molecule Hedgehog Inhibitor and miRNA for Treating Pancreatic Cancer

Virender Kumar[†], **Goutam Mondal**[†], **Paige Slavik**[†], **Satyanarayna Rachagani**[‡], **Surinder K. Batra**[‡], and **Ram I. Mahato**[*,†]

[†]Department of Pharmaceutical Sciences, University of Nebraska Medical Center, 986025 Nebraska Medical Center, Omaha, Nebraska 68198, United States

[‡]Departments of Biochemistry and Molecular Biology, University of Nebraska Medical Center, 986025 Nebraska Medical Center, Omaha, Nebraska 68198, United States

Abstract

Successful treatment of pancreatic ductal adenocarcinoma (PDAC) remains a challenge due to the desmoplastic microenvironment that promotes both tumor growth and metastasis and forms a barrier to chemotherapy. Hedgehog (Hh) signaling is implicated in initiation and progression of PDAC and also contributes to desmoplasia. While Hh levels are increased in pancreatic cancer cells, levels of tumor suppressor miR-let7b, which targets several genes involved in PDAC pathogenesis, is downregulated. Therefore, our overall objective was to inhibit Hh pathway and restore miR-let7b simultaneously for synergistically treating PDAC. miR-let7b and Hh inhibitor GDC-0449 could inhibit the proliferation of human pancreatic cancer cells (Capan-1, HPAF-II, T3M4, and MIA PaCa-2), and there was synergistic effect when miR-let7b and GDC-0449 were coformulated into micelles using methoxy poly(ethylene glycol)-*block*-poly(2-methyl- 2-carboxyl-propylenecarbonate-*graft*-dodecanol-graft-tetraethylene-pentamine) (mPEG-*b*-PCC-*g*-DC-*g*-TEPA). This copolymer self-assembled into micelles of <100 nm and encapsulated hydrophobic GDC-0449 into its core with 5% w/w drug loading and allowed complex formation between miR-let7b and its cationic pendant chains. Complete polyplex formation with miRNA was observed at the N/P ratio of 16/1. Almost 80% of GDC-0449 was released from the polyplex in a sustained manner in 2 days. miRNA in the micelle formulation was stable for up to 24 h in the presence of serum and high uptake efficiency was achieved with low cytotoxicity. This combination therapy effectively inhibited tumor growth when injected to athymic nude mice bearing ectopic tumor generated using MIA PaCa-2 cells compared to micelles carrying GDC-0449 or miR-let7b alone. Immunohistochemical analysis revealed decreased tumor cell proliferation with increased apoptosis in the animals treated with miR-let7b and GDC-0449 combination.

[*]**Corresponding Author:** Phone: (402) 559-5422. Fax: (402) 559-9543. ram.mahato@unmc.edu.

Supporting Information

Design of amphiphilic copolymer for codelivery of GDC-0449 and miR-let7b for treating for pancreatic cancer, refractive index-gel permeation chromatography (RI-GPC) traces of mPEG-*b*-PCC-*g*-DC-*g*-TEPA copolymer and specifics of molecular weight data and characteristics, plot of fluorescence intensity of pyrene vs logarithm of mPEG-*b*-PCC-*g*-DC-*g*-TEPA copolymer, particle size distribution of GDC-0449 encapsulated micelles using dynamic light scattering. This material is available free of charge via the Internet at http://pubs.acs.org.

Notes

The authors declare no competing financial interest

Graphical abstract

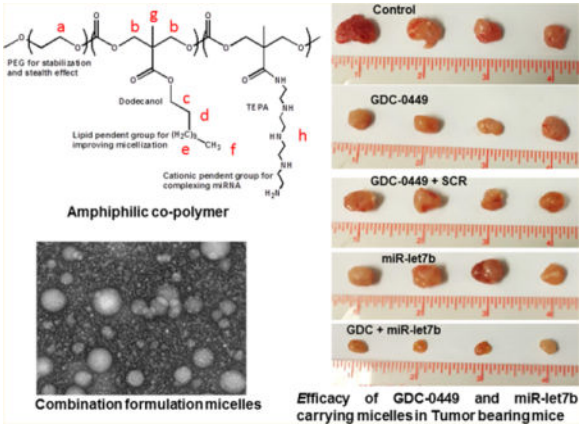

Keywords

GDC-0449; Hh signaling; K-RAS; micelles; miR-let7b; pancreatic ductal adenocarcinoma

1. INTRODUCTION

Pancreatic ductal adenocarcinoma (PDAC) is a leading cause of cancer related mortality, with a dismal 2–5% five year survival rate.[1] Because of its late stage clinical manifestation, 85% of patients have metastatic disease at the time of diagnosis, making surgical and therapeutic interventions ineffective. The current FDA approved chemotherapeutic agent for pancreatic cancer is gemcitabine, which provides only symptomatic improvement in a lesser proportion of patients. New combination therapy FOLFIRINOX (fluorouracil [5-FU], leucovorin, irinotecan, and oxaliplatin) showed improvement compared to gemcitabine alone; however, there was a significant rate of grade 3/4 toxicity in PDAC patients.[2]

PDAC is characterized by a dense desmoplastic/stromal reaction that consist of largely fibroblasts, pancreatic stellate cells (PSCs), and extracellular matrix (ECM) proteins including collagen I and fibronectin. PSCs form a niche for cancer stem cells (CSCs) and promote their self-renewal and invasiveness. CSCs are a subset of cancer cells that not only drive tumor growth but also resistant to chemotherapy and radiation. Hedgehog (Hh) signaling promotes desmoplasia causing PSC differentiation into myofibroblasts that result in poor delivery of therapeutic agents. Hh ligands also facilitate the maintenance of CSCs.[3] Blocking the Hh pathway decreases desmoplastic reactions, eliminates CSCs, and increases tumor vascular density, thus ultimately improves the chemotherapy.[4] Vismodegib (GDC-0449) antagonizes Hh signaling by inhibiting the smoothened (SMO) and Shh-Gli signaling selectively.[5] However, its clinical benefits are limited due to its poor aqueous solubility and low bioavailability.

miRNAs are endogenous noncoding single stranded RNAs of 19–24 nt that regulate gene expression through mRNA cleavage or translational inhibition. miRNA plays a crucial role in the initiation, progression, and maintenance of CSCs. Pancreatic CSCs express differential levels of miR-99a, miR-100, miR-125b, miR-192, and miR-429 compared with

controls and miR-200c, miR-203, and miR-183 activity can lead to the downregulation of stem cell factors.[6,7] Expression levels of miRNAs correlate well with drug resistance, invasion, metastasis, and epithelial to mesenchymal transition (EMT).[8] Despite their promise, the clinical potential of miRNAs has not been realized, owing to the challenges involved in their in vivo delivery. Several barriers such as serum instability, nonspecific accumulation, improper intracellular release, and rapid excretion limit the clinical application of therapeutic miRNAs. Further, miRNAs are highly hydrophilic, which decreases their extravasation into the desmoplasmic PDAC tissue. Previous studies including our own show that miR-let7b is downregulated in pancreatic cancer cells and primary pancreatic cancer.[9,10] miR-let7b can target several tumor-promoting genes including K-RAS, MUC4, NCOA3, HMGA2, TGFβR1, and STAT3 phosphorylation[11–13] thus its restoration can inhibit PDAC growth and progression.

A combination of two drugs having different mechanisms of action can inhibit tumor progression with synergistic or additive effects.[14–16] Previously, we have synthesized cationic polymer mPEG-*b*-PCC-*g*-GEM-*g*-DC-*g*-CAT for simultaneous delivery of miR-205 and gemcitabine, where gemcitabine was covalently attached to polymer backbone.[17] However, GDC-0449 has no functional group for chemical conjugation to the polymer. Therefore, in this study, we synthesized methoxy poly(ethylene glycol)-*block*-poly(2-methyl-2-carboxyl-propylene carbonate-*graft*-dodecanol-graft tetraethylpentamine) (mPEG-*b*-PCC-*g*-DC-*g*-TEPA) which can self-assemble in micelles, form complex with miR-let7b, and encapsulate GDC-0449. These micelles were characterized for particle size, ζ potential, drug loading, miRNA complexation, stability, and transfection efficiency. The formulations were tested for the effect on proliferation of pancreatic cancer cell lines (HPAF-II, T3M4, CAPAN-1, and MIAPaCa-2). Finally, these formulations were injected into subcutaneous pancreatic tumor bearing mice to determine whether there is synergism between these two drugs in inhibiting tumor growth.

2. MATERIALS AND METHODS

2.1. Materials and Reagents

Benzyl bromide, 2,2-bis(hydroxymethyl)propionic acid, methoxy poly(ethylene glycol) (mPEG, M_n = 5000, PDI = 1.03), and stannous 2-ethylhexanoate ($Sn(Oct)_2$) were purchased from Sigma-Aldrich (St. Louis, MO). Tetraethylenpentamine and dodecanol were purchased from Alfa-Aesar (Ward Hill, MA). TaqMan reverse transcription reagent kit was purchased from Life Technologies (Grand Island, NY). Radioimmunoprecipitation assay (RIPA) buffer and SYBR green-1 were purchased from (Roche, Indianapolis, IN). miR-let7b (mature sequence UGAGGUAGUAGGUUGUGUGGUU) and scrambled miRNA were purchased from Invitrogen (Carlsbad, CA). All other reagents were purchased from Sigma-Aldrich and used without further purification.

2.2. Synthesis of Copolymer

To synthesize mPEG-*b*-PCC-*g*-DC-*g*-TEPA copolymer, monomer 2-methyl-2-benzyloxycarbonyl-propylene carbonate (MBC) was synthesized by reacting 2,2-bis(hydroxymethyl)propionic acid with benzyl bromide for 16 h under nitrogen at 100 °C.[18]

mPEG-MBC was synthesized by ring opening polymerization in the presence of $Sn(Oct)_2$ as a catalyst at 100 °C 8 h. mPEG-MBC was then dissolved in tetrahydrofuran (THF):methanol (1:1, v/v) and hydrogenated in the presence of 10 wt % palladium on carbon to obtain the copolymer containing carboxyl pendant groups (mPEG–PCC).[19] Finally, tetraethylepentamine (TEPA) and dodecanol were conjugated by carbodiimide coupling reaction at room temperature for 48 h to obtain mPEG-*b*-PCC-*g*-DC-*g*-TEPA. This final product was purified by repeated precipitation in isopropyl alcohol followed by diethyl ether. mPEG-*b*-PCC-*g*-DC-*g*-TEPA was characterized using ^{1}H NMR (Bruker 400 MHz) after dissolving in DMSO-d_6.

2.3. Preparation of Micelles

Micelles encapsulating GDC-0449 and complexing miR-let7b were formulated by the film hydration method as reported earlier with slight modifications.[17] Briefly, 20 mg of mPEG-*b*-PCC-*g*-DC-*g*-TEPA was dissolved in chloroform in a glass vial, and a thin film was formed by solvent evaporation under reduced pressure. Chloroform was removed completely by placing the vial overnight in a vacuum desiccator. miR-let7b was added to 1 mL of HEPES buffer (10 mM, pH 6.5) and mixed gently. HEPES buffer containing miR-let7b was then added to the copolymer film and vortexed for 5 min. Suspension was shaken for 30 min at 37 °C to enable miRNA complexation. Formulation was then centrifuged at 5000*g* for 5 min and filtered using a 0.22 μm filter (Millipore) and lyophilized. miR-let7b and GDC-0449 combination formulations were prepared by dissolving the drug and copolymer in chloroform and then followed by film formation and hydration with HEPES buffer containing miR-let7b.

2.4. Characterization of Formulations

Micelles carrying miR-let7b and GDC-0449 were characterized for particle size distribution and ζ potential using Malvern Zetasizer (NanoZS Series) and for morphology using transmission electron microscope (TEM). Micelles containing miRNA and used for particle size characterization or drug release were formulated at N/P ratio of 32:1. Micellar drug loading was measured by HPLC-UV as reported earlier.[20] To determine the critical micelle concentration (CMC) of cationic copolymer, pyrene fluorescence was used as described previously.[21] From pyrene stock solution of 2.6 mg/mL in chloroform, 19.23 μL (50 μg pyrene) aliquots were transferred to a series of clean, dry glass vials. Solvent was evaporated under vacuum while protected from light. Copolymer solutions were prepared at concentrations ranging from 1×10^{-9} to 1.0 mg/mL in distilled water and added to each dry pyrene vials to obtain the final concentration of 6.18×10^{-5} M. Vials containing mixtures were shaken for 24 h at room temperature in dark. Undissolved pyrene was removed by filtration, and pyrene concentration solubilized in the micelles was determined by spectrofluorometer at wavelengths of excitation 339 nm and emission at 390 nm.

To determine GDC-0449 release, formulation containing 0.5 mg of GDC-0449 was placed in a dialysis bag (MWCO 1000 Da) and suspended in PBS (pH 7.4) containing Tween 80 (1.0% w/v) at room temperature. Then 1 mL samples at a regular interval were withdrawn and replaced with fresh media (PBS + 1.0% Tween 80). Samples were analyzed using HPLC. Drug release was determined in the absence and presence of miR-let7b.

Agarose gel retardation assay was used to evaluate miR-let7b condensation. Copolymer/miR-let7b complexes were prepared at different N/P ratios ranging from 4 to 64, and the complexes containing 1× loading buffer were loaded onto 1% agarose gel premixed with 0.05 mg/mL ethidium bromide. The mixture was separated in 1× Tris/borate/EDTA (TBE) buffer at 100 V for 30 min. miR-let7b bands were visualized using an UV GelDoc EZ system (Bio-Rad, Hercules, CA).

miRNA release from GDC-0449 encapsulated and miR-let7b complexed micelles (N/P ratio: 32/1) was determined using heparin polyanion competition. Heparin sodium was added to miR-let7b at different weight ratios (0, 4, 8, 16, 32, and 64 μg) in 10 μL of PBS were added to the nanocomplex suspension and incubated at room temperature for 45 min. The miRNA released from the complex was analyzed by gel electrophoresis. miRNA stability within nanocomplexes was determined by incubating the complexes (N/P ratio: 32/1) in 25% fetal bovine serum (FBS) for different time points at 37 °C. After indicated time points, complexes were taken out and then incubated with heparin sulfate solution for 45 min. The mixture was then electrophoresed.

2.5. Transfection Efficiency

MIA PaCa-2 cells were seeded into Nunc Chamber slides (Lab-Tek, Rochester, NY) at a density of 4×10^4 cells/well in serum-free DMEM for Lipofectamine 2000 and DMEM with 10% serum for transfection with nanocomplex for 24 h. Copolymer/Block-IT fluorescent oligo complexes were prepared at the N/P ratio of 32:1. Lipofectamine transfection was carried out as per the manufacturer's instructions, and these cells were considered as the control. Nanocomplexes were added to respective wells (oligo 20 pmol/well) with gentle shaking and incubated for 3h at 37 °C. Cells were then washed twice with PBS containing Ca^{2+} and Mg^{2+} and fixed with 10% paraformaldehyde (PFA) in PBS for 15 min at room temperature. After fixing, cells were observed under a fluorescent microscope (Zeiss, Jena, Germany) and images were recorded.

2.6. Endosomal Escape Study

Cells were plated in Nunc Chamber slides at a density of 40000 cells/well in 300 μL of DMEM. CellLight Early Endosomes-GFP was added for staining the endosomes as per the manufacturer's instructions. After overnight incubation, 50 μL of nanocomplexes (20 μM) formulated from fluorescent Block-IT oligo were added to each well. After incubation for certain time points, cells were fixed with 10% PFA. For each time point, images were captured using Endosomes-GFP channel (excitation 488 nm, band-pass filter 500–550 nm) and Block-IT channel (excitation 543 nm, bandpass filter 560–615 nm). Image processing and analysis was conducted with ZEN software (Zeiss, Jena, Germany).

2.7. Cell Viability Assay

Cytotoxicity of the micelles carrying GDC-0449 and miR-let7b was determined by carrying out the cell viability assays. HPAF-II, M3T4, Capan-1, and MIA PaCa-2 cells (5000 cells/well) were seeded 24 h before transfection. Transfection was carried out using micelles carrying GDC-0449 (1–10 μM) and constant miR-let7b (10 pmol) concentration. Micelles carrying scrambled miRNA and GDC-0449 formulations were used as the positive control.

Cell viability was assessed after 48 h by MTT assay using a microplate reader (Epoch, BioTek Instruments Inc., Winooski, VT).

$$\text{cell viability } \% = \frac{\text{absorbance test}}{\text{absorbance control}} \times 100 \quad (1)$$

2.8. In Vivo Study

All animal experiments were performed in accordance to the protocol approved by the Institutional Animal Care and Use Committee (IACUC) at the University of Nebraska Medical Center (UNMC, Omaha, NE). Flank tumors were established in 8–10 week old male athymic nude mice by subcutaneous injection of 3×10^6 MIA PaCa-2 cells suspended in a total 200 μL of 1:1 serum-free media and Matrigel (BD Biosciences, CA). When the tumor volume reached 200–300 mm^3, animals were randomly divided into five groups (n = 5): blank micelles, micelles containing GDC-0449, GDC-0449 and scrambled miRNA (SCR), micelles containing miR-let7b, and micelles carrying miR-let7b and GDC-0449. Formulations were administered intratumorally thrice a week for 2 weeks at an equivalent dose of 10 mg/kg GDC-0449 and 2 mg/kg miR-let7b or the negative control (NC). Tumor size was measured at regular intervals using digital vernier caliper. Body weight of the animals was recorded thrice a week. At the end of the study, tumor tissues were excised, weighed, and either fixed in formaldehyde or snapped frozen for further analysis.

2.9. Real-Time RT-PCR

Gene expression levels of downstream targets of miR-let7b and GDC-0449 were determined using real-time RT-PCR. Total RNA from specimens was extracted using RNeasy RNA isolation kit (Qiagen, MD) as per manufacturer's protocol. mRNA was then reverse transcribed into cDNA using TaqMan qRT-PCR kit (Life Technologies, Carlsbad, CA). cDNA templates were then amplified by real-time PCR on a Light Cycler 480 (Roche, Indianapolis, IN) using SYBR Green dye universal master mix. Primer sequences used were Shh (forward, CCAGAAACTCCGAGCGATTTA; reverse, TTTCACCGAGCA GTG GATATG) and GLI-1 (forward, CTACATCAACTCCGGCCAATAG; reverse, GGT TGGGAGGTAAGGATCAAAG). β-actin (primer sequence forward, AGCCATGTACGTTGCTATCC; reverse, CGTAGCACAGCTTCTCCTTAAT) was used as a housekeeping gene and relative amount of mRNA was calculated using Crossing point (Cp) values.

2.10. Western Blot

Total proteins from tissues were extracted by homogenizing in RIPA buffer premixed with protease inhibitor cocktail (Sigma, St. Louis, MO). Proteins concentrations were determined using a BCA protein assay kit (Thermo Scientific, Rockford, IL). Total protein (50 μg) was separated on 12% mini PROTEAN polyacrylamide gels and then transferred to polyvinylidenefluoride (PVDF) (Life Technologies Carlsbad, CA) using iBlot gel transfer system. Membrane was blocked using Odyssey blocking buffer for 1 h at room temperature. Membranes were incubated overnight with rabbit polyclonal to Gli-1 (SC-20687), rabbit polyclonal to Shh (SC-h160), goat polyclonal to β-actin (SC-1616) (1:1000) (Santa Cruz

Biotech., Dallas, TX), and mouse monoclonal antibodies against KRAS (ab-55391) (1:1000) (Abcam, Cambridge, MA). After washing with TBST buffer, the membrane was further incubated with their corresponding antirabbit, antigoat, and antimouse IR dye conjugated secondary antibodies (1:10000) (LI-COR Biosciences, Lincoln, NE) for 60 min and visualized using LI-COR imaging system. Expression levels of desired protein were normalized against β-actin (SC-1616) protein expression levels.

2.11. Histochemical and Immunofluorescence Assays

Tumors were excised and specimens were fixed in 10% PFA overnight and embedded in paraffin. To evaluate tissue morphology, sections (4 μm) were stained with hematoxylin and eosin (H&E) and then analyzed blindly. For cell proliferation marker Ki-67, sections were probed with rabbit polyclonal Ki-67 antibody (1:50) (ab-15580). Sections were incubated for 45 min at room temperature with antirabbit horse raddish peroxidase (HRP) conjugated secondary antibody diluted to 1:500 in 2% BSA/1× PBS solution. All stained slides were visualized under microscope (Leica, Germany).

2.12. Terminal Deoxynucleotidyl Transferase Nick End Labeling (TUNEL) Staining

DeadEnd fluorometric TUNEL staining to identify apoptotic cells by fluorescein-12–dUTP labeling of fragmented DNA was carried out as per manufacture's protocol (Promega). Briefly, paraffin-embedded tumor tissue sections were deparaffinized by immersing in xylene and rehydrated by sequentially immersing the slides through graded ethanol. After washing with PBS, sections were fixed with 5% formaldehyde, washed with PBS, and permeabilized by incubating with Proteinase K solution for 15 min. After fixing with 5% PFA and washing, slides were covered with 100 μL of equilibration buffer for 15 min and washed with PBS. Subsequently, slides were coated with rTdT incubation buffer (equilibration buffer + nucleotide mix + rTdT enzyme) and incubated at 37 °C for 60 min. For the negative control, incubation buffer was prepared without rTdT enzyme and incubated. Slides were then washed with 1× SSC buffer and PBS and incubated in 1 μg/mL propidium iodide (PI) in PBS for 20 min. Finally, slides were washed with deionized water twice and observed under confocal microscope.

2.13. Statistics

Student's unpaired t test was used to compare the mean values of individual groups. A p value <0.05 was considered as statistically significant.

3. RESULTS

Micelles containing miR-let7b and GDC-0449 were formulated and evaluated both in vitro and in vivo for treating pancreatic cancer. We have complexed hydrophilic miR-let7b and encapsulated hydrophobic GDC-0449 in our cationic polymeric micelles.

3.1. Copolymer Synthesis and Characterization

Cationic amphiphilic copolymer was synthesized by attaching DC and TEPA to methoxypoly(ethylene glycol)-*block*-poly(2-methyl-2-carboxyl-propylene carbonate) (PEG–PCC) by carbodiimide coupling (Supporting Information, Figure S1A). mPEG–PCC was

characterized with ^{1}H NMR and showed copolymer backbone peaks corresponding to PEG(–CH_2–CH_2–O) at δ 3.5, PCC (–CH_2–) at δ 4.2. After hydrogenation, the characteristic peak of phenyl ring at δ 7.3 disappeared and a peak at δ 13 corresponding to exposed carboxyl group was observed which indicates the complete removal of pendant benzyl group.[19] On the basis of the peak integrals of mPEG and PCC protons, a number-average molecular weight (M_n) of mPEG–PCC copolymer was calculated to be 10370 g/mol with 31 PCC units. EDC/HOBt coupling reaction was used to conjugate DC and TEPA chains to the copolymer. ^{1}H NMR characterization showed peaks for TEPA at δ7–8 (–CO–NH–) and DC peaks at δ of 1–2 (CH_2) (Supporting Information, Figure S1B). The degree of polymerization (DP) of copolymer was calculated based on ^{1}H NMR integration ratio of peaks assigned at δ 3.63 to ethylene protons of PEG backbone. Approximately 12 units of DC and 8 units of TEPA were present in final copolymer with disappearance of COOH peak and M_n calculated was approximately 14000 g/mol. Gel permeation chromatography of the copolymer showed a unimodal peak with weight-average of 13776 g/mol (PDI of 2.0) (Supporting Information, Figure S2).

3.2. Formulation Characterization

Mean particle sizes of micelles encapsulating GDC-0449 or in combination with miRNA were measured using DLS and TEM (Figure 1A,B and Supporting Information, Figure S4). Micelles encapsulated only GDC-0449 showed a mean size of 95 ± 10 nm (with PDI 0.11), while there was a slight decrease in the mean size (80 ± 10 nm) (with PDI 0.10) when micelles contained both GDC-0449 and miRNA. TEM showed the morphology of GDC-0449 loaded miR-let7b complexed micelles as well dispersed spherical particles. Compared to the hydrated state in DLS size of micelles (80 ± 10 nm), TEM was carried out in the dried state, resulting in small size particles (60 ± 10 nm). Zeta potential of miR-let7b polyplexed micelles was in the range of 5 ± 2 mV compared to −15 ± 2 mV for free miR-let7b solution. The CMC value of copolymer in the aqueous system as determined using pyrene was 5.5×10^{-4} (g/L) (Supporting Information, Figure S3). These micelles carrying GDC-0449 and miR-let7b were fairly stable at room temperature, and there was little change in their particle size distribution even after a week (data not shown). Also, there was little release of miRNA from the polyplex, suggesting the high stability of this formulation. mPEG-*b*-PCC-*g*-DC-*g*-TEPA significantly increased solubility of GDC-0449 up to 1560 ± 50 μg/mL, as determined by HPLC-UV. GDC-0449 release in the presence and absence of miRNA from the combination formulations was determined at pH 7.4. Drug release study showed a controlled release of 80% in 2 days, with no effect of the presence of miR-let7b on GDC-0449 release from the polyplexes (Figure 1C).

To determine the effect of N/P ratio on miR-let7b complexation, miR-let7b was complexed with mPEG-*b*-PCC-*g*-DC-*g*-TEPA at N/P ratios ranging from 1:1 to 64:1. Complete retardation of miRNA was observed at N/P ratio of 32:1 (Figure 1D). Heparin (170U/mg) was able to dissociate miR-let7b from the polyplexes at the ratio of 1:16 (Figure 1E). miR-let7b was stable in 25% FBS for 24 h when formulated in micelles, while naked miRNA degraded within 1h (Figure 1F), suggesting polyplex formation stabilizes miRNA against exonucleases.

3.3. Uptake Efficiency and Lysosomal Escape

Cellular uptake and intracellular distribution of these micelles were evaluated by confocal laser scanning microscopy. Although our cationic polymer showed transfection efficiency similar to Lipofectamine 2000 (Figure 2), significantly lesser cytotoxicity was observed based on the N/P (±) ratio of the complexes. Also, uptake study using our formulation was carried out using serum containing media unlike Lipofectamine 2000 lipoplexes which required serum-free media for transfection. The N/P ratio of lipofectamine: miR-let7b was ~22:1 while our polymer was nontoxic even at N/P ratio of 64:1.

For endosomal escape study, MIA PaCa-2 cells were labeled with GFP and transfected with Cy3 labeled oligonucleotide formulation for different time points. After 1 h of incubation, the colocalization of both fluorescent signals were observed, suggesting efficient uptake of micelles by the cells (Figure 3A). Majority of fluorescence was localized in endosomal compartments and after 3 h, both fluorescent colors were separated and clearly showed that micelles were not restricted to early endosomes (Figure 3B), indicating its potential to be used as a miRNA carrier.

3.4. Cell Viability Study

Cytotoxicity of micelles carrying GDC-0449 and miR-let7b were determined at N/P ratios of 32:1 with 10 pmol miR-let7b. Cell viability was determined by MTT assay after 48 h of incubation and compared to the cells incubated with micelles carrying either GDC-0449 or miR-let7b alone or GDC-0449 and scrambled miRNA. The combination formulations reduced cell viability to 47% in HPAF-II, 20% in Capan-I, 30% in T3M4, and 37% in MIA PaCa-2 cells at the dose of 10 pmol miR-let7b and 10 μM GDC-0449, while both miR-let7b and GDC-0449 monotherapy failed to kill cells at the low doses (Figure 4). Therefore, combination formulation was quite effective, leading to a significant decrease in cell viability, suggesting synergism between these two drugs.

3.5. In Vivo Evaluation

The in vivo efficacy of micelles containing miR-let7b and GDC-0449 was determined in subcutaneous tumor bearing athymic nude mice generated using MIA PaCa-2 cells. All the animals did not show any signs of toxicity or loss in body weight during the treatment period (Figure 5A). All the treatment groups had significantly low tumor growth compared to the control group (537.30 ± 38.43 mm^3). However, significant tumor growth inhibition was observed in the mice which received micelles carrying miR-let7b and GDC-0449 (119.07 ± 13.25 mm^3) compared to the formulations containing miR-let7b (350.35 ± 64.15 mm^3) or GDC-0449 alone (249.19 ± 32.74) or formulations containing GDC-0449 and SCR miRNA (285.12 ± 58.63 mm^3) (Figure 5B,C).

RT-PCR was used to determine mRNA expression of Shh and Gli-1 in tumor tissues where relative expression of Shh mRNA was inhibited by GDC-0449 and GDC-0449 + SCR treatment groups to 59.15% ± 10.19 and 69.07% ± 10.86, respectively, wherein its levels were 47.62% ± 7.05 in the combination treatment group. Relative Gli-1 mRNA also displayed the similar trend, where its transcripts were decreased to 63.45% ± 5.64 and 68.65% ± 3.03 by GDC-0449 and GDC-0449 + SCR formulations, respectively, and up to

31.82% ± 2.47 reductions by the combination treatment group (Figure 6A). We did not observe any significant reduction in level of either of these transcripts in mice treated with the formulations containing miR-let7b alone. Western blot analysis shows reduced Gli-1 and K-RAS protein expression in treatment groups (Figure 6B).

Immunohistochemical analysis of tumor sections revealed that the treated mice displayed lower Ki-67 staining compared to untreated mice. Among treatment groups, mice treated with combination therapy had least Ki-67 staining (Figure 7A). Treatment with micelles carrying GDC-0449 and miR-let7b resulted in loosened groups of epithelial cells, whereas the control group had dense cells within tumor mass (Figure 7B). Tumor sections were examined for apoptosis of cancer cells using TUNEL assay. No apoptotic (TUNEL-positive green fluorescent) cells were observed in sections from the control mice. Mice treated with micelles containing miR-let7b or GDC-0449 alone showed only modest increase in the number of apoptotic cells, while miR-le7b and GDC-0449 combination therapy significantly enhanced apoptosis (Figure 7C).

4. DISCUSSION

PDAC is among the most lethal human cancers and poses medical challenge due to its insensitivity to the majority of proven chemotherapeutic agents. Hh signaling promotes proliferation of most cancer cell types including breast cancer, prostate cancer, colon cancer, brain tumors, pancreatic cancer, and basal cell carcinomas.[22–27] Hh signaling controls EMT, enhances cell proliferation by MAPK- and PI3-kinase-dependent manner, decreases apoptosis by regulation of Bcl-2 and Bcl-X, and also proliferates CSCs. Hh pathway also promotes cell invasion, migration, and chemoresistance.[28,29] By inhibiting Hh signaling, GDC-0449 has shown the potential of reducing tumor cell growth.[30]

GDC-0449 and miR-let7b represent diverse physicochemical properties, with GCD-0449 being a hydrophobic small molecule while miR-let7b is an oligonucleotide with high aqueous solubility. Therefore, we have synthesized an amphiphilic cationic mPEG-*b*-PCC-*g*-DC-*g*-TEPA copolymer, which self-assembles into micelles (and thus can encapsulate GDC-0449 and bears pendant cationic chains to form complexes with miR-let7b. Apart from codelivery, our system offers distinct advantages in terms of (a) PEG corona on the polymer imparting stealth property, (b) small size of these micelles can take advantage of the EPR effect to maximize drug delivery to pancreatic tumor, and (c) codelivery will ensure similar biodistribution profiles of both the active therapeutic moieties. Further, these nanomedicines are stable and scalable and hence bear high translational potential.

While miR-let7b has been reported to retard pancreatic cancer cell growth and proliferation in vitro, it failed to inhibit PDAC progression in vivo due to the lack of efficient delivery.[31] Therefore, there is a great need to develop an efficient delivery system for miRNAs. We complexed miR-let7b with cationic chains of mPEG-*b*-PCC-*g*-DC-*g*-TEPA copolymeric micelles. This copolymer self-assembles into micelles and encapsulates GDC-0449 into its core and allows complex formation between miR-let7b and cationic pendant chains. The entrapment of miR-let7b into these micelles offers advantages of its improved in vivo stability, enhanced mean residence time, and ensuring similar biodistribution of both

GDC-0449 and miR-let7b. Cells of reticuloendothelial system (RES) recognize particles of large size, while particles smaller than 200 nm manage to escape. The mean particle size of our polyplexes ranged from 80 to 100 nm with spherical morphology (Figure 1A,B). Moreover, mPEG corona on the polymer imparts stealth property for longer mean residence time at the tumor site.[32] By micellization, the aqueous solubility of GDC-0449 was increased from 0.1 to 1560 ± 50 μg/mL.

Efficient miR-let7b complexation with the copolymer primary amines was observed at N/P ratio of 16/1 (Figure 1D). Low ζ potential value of the formulations suggests that PEG corona surrounds the polyplex core.[33] Decrease in polyplex mean particle size was observed in the DLS analysis after miRNA addition may be due to the strong interaction between miRNA and cationic chains, leading to decrease in interchains force of repulsion.[34] Complete displacement of miRNA from polyplexes were observed in the presence of polyanionic heparin, demonstrating that miRNA can be effectively released from the carrier (Figure 1E). Serum stability study shows that the naked miRNA degraded within 6 h of incubation, while miRNA in formulation was stable up to 24 h (Figure 1F).

We determined the effect of GDC-0449 and miR-let7b formulations on cell viability using four pancreatic cancer cell lines known to express high levels of Hh ligands.[35] miR-let7b or GDC-0449 alone in formulations was ineffective in reducing cell viability, whereas cytotoxicity was increased significantly when GDC-0449 and miR-let7b were used as combination formulations (Figure 4). This synergy may be due to the fact that Hh signaling pathway works cooperatively with K-RAS in pancreatic cancer.[36] Thus, GDC-0449 reduces proliferation and induces apoptosis of these cells via Gli-1 dependent manner and chemosensitizes them to anti-K-RAS miR-let7b.

In vivo efficacy of the formulations was evaluated in athymic nude mice bearing ectopic tumor generated by subcutaneous implantation of MIA PaCa-2 cells. Treatment of these mice with micelles carrying miR-let7b and GDC-0449 resulted in a significant reduction in tumor growth rate and tumor weight compared to the control group (Figure 5B,C). There was significant reduction in Shh and Gli-1 expression as analyzed by RT-PCR and K-RAS expression as analyzed by Western blot (Figure 6).

We observed a high expression of proliferation marker Ki-67 in control group showing a high cell growth, whereas treatment with miR-let7b and GDC-0449 combination reduced cellular proliferation to a significantly low level (Figure 7A). Histological analysis of tumor specimens revealed a compact mass of epithelial cells in the control group, whereas combination treatment tumors appeared as loose epithelial cell aggregates with a larger amount of interspersed mesenchymal cells (Figure 7B), which is in line with the literature.[36] TUNEL assays demonstrated that GDC-0449 and miR-let7b treatment resulted in increased number of apoptotic cells compared with the control or single drug treated groups (Figure 7C).

All of these observations conclude that by combining K-RAS targeting tumor suppressor miR-let7b with Hh inhibitor GDC-0449 reduces tumor growth synergistically. Although the precise mechanisms of this cooperation are subject to further investigation, it appears that

inhibition of Hh signaling sensitizes tumor cells to anti K-RAS therapy. This is in line with previous studies, where Hh pathway activation reduced sensitivity to treatment with therapeutics that target K-RAS signaling pathway. Further, targeting both Hh and anti-K-RAS pathways reduced pancreatic tumor initiation and growth.[37]

We are aware of the outcome of a recent clinical trial, which revealed remarkable decrease in Shh and proliferation marker Ki-67 after treatment with GDC-0449, but the combination of GDC-0449 and gemcitabine failed to improve the median survival of pancreatic cancer patients.[38] Furthermore, in a separate study, aggressive and undifferentiated tumor growth upon Hh deletion has been reported.[39,40] This tumor-promoting effect of Hh signaling suppression may be due to increased angiogenesis within tumor mass by very high dose of GDC-0449 used (100 mg/kg).[41] This is because, in a different clinical study, GDC-0449 in combination with gemcitabine and nab-paclitaxel showed higher overall survival compared to gemcitabine plus nab-paclitaxel.[42] Therefore, successful inhibition of tumor growth requires a delicate balance between the beneficial and harmful effects of Hh signaling.

5. CONCLUSIONS

In conclusion, we demonstrated that mPEG-*b*-PCC-*g*-DC-*g*-TEPA efficiently encapsulates GDC-0449 and forms complexes with miR-let7b, and this combination therapy has the potential to inhibit pancreatic cancer both in vitro and in vivo. This combination formulation represents a promising therapeutic approach to treat advanced pancreatic cancer with dense desmoplasia.

Supplementary Material

Refer to Web version on PubMed Central for supplementary material.

Acknowledgments

The National Institutes of Health (1R01EB017853), Fred and Pamela Buffet Cancer Center, and Cattlemen's Ball of Nebraska, Inc., and the Faculty Start-up fund are duly acknowledged for providing financial support for this work.

ABBREVIATIONS USED

CSCs	cancer stem cells
CMC	critical micelle concentration
DIPEA	*N,N*-diisopropylethylamine
ECM	extracellular matrix
EMT	epithelial to mesenchymal transition
Hh	hedgehog
H&E	hematoxylin and eosin
HRP	horse radish peroxidase
K-RAS	Kirsten rat sarcoma

MBC	2-methyl-2-benzyloxycarbonyl-propylene polyethylene glycol
miR-let7b	miRNA-Let7b
MUC-4	mucin-4
NMR	nuclear magnetic resonance
PDAC	pancreatic ductal adenocarcinoma
PSCs	pancreatic stellate cells
RES	reticuloendothelial system
RT-PCR	reverse transcription polymerase chain reaction
SMO	smoothened
Shh	sonic hedgehog
TGF-β	transforming growth factor beta
GDC-0449	Vismodegib

References

1. Wolfgang CL, Herman JM, Laheru DA, Klein AP, Erdek MA, Fishman EK, Hruban RH. Recent progress in pancreatic cancer. CA: Cancer J Clin. 2013; 63:318–348. [PubMed: 23856911]
2. Mohammed S, Van Buren G II, Fisher WE. Pancreatic cancer: advances in treatment. World J Gastroenterol. 2014; 20:9354–9360. [PubMed: 25071330]
3. Huang FT, Zhuan-Sun YX, Zhuang YY, Wei SL, Tang J, Chen WB, Zhang SN. Inhibition of hedgehog signaling depresses self-renewal of pancreatic cancer stem cells and reverses chemoresistance. Int J Oncol. 2012; 41:1707–1714. [PubMed: 22923052]
4. Olive KP, Jacobetz MA, Davidson CJ, Gopinathan A, McIntyre D, Honess D, Madhu B, Goldgraben MA, Caldwell ME, Allard D, Frese KK, Denicola G, Feig C, Combs C, Winter SP, Ireland-Zecchini H, Reichelt S, Howat WJ, Chang A, Dhara M, Wang L, Ruckert F, Grutzmann R, Pilarsky C, Izeradjene K, Hingorani SR, Huang P, Davies SE, Plunkett W, Egorin M, Hruban RH, Whitebread N, McGovern K, Adams J, Iacobuzio-Donahue C, Griffiths J, Tuveson DA. Inhibition of Hedgehog signaling enhances delivery of chemotherapy in a mouse model of pancreatic cancer. Science. 2009; 324:1457–1461. [PubMed: 19460966]
5. De Smaele E, Ferretti E, Gulino A. Vismodegib, a small-molecule inhibitor of the hedgehog pathway for the treatment of advanced cancers. Curr Opin Invest Drugs. 2010; 11:707–718.
6. Tanase CP, Neagu AI, Necula LG, Mambet C, Enciu AM, Calenic B, Cruceru ML, Albulescu R. Cancer stem cells: involvement in pancreatic cancer pathogenesis and perspectives on cancer therapeutics. World J Gastroenterol. 2014; 20:10790–801. [PubMed: 25152582]
7. Wellner U, Schubert J, Burk UC, Schmalhofer O, Zhu F, Sonntag A, Waldvogel B, Vannier C, Darling D, zur Hausen A, Brunton VG, Morton J, Sansom O, Schüler J, Stemmler MP, Herzberger C, Hopt U, Keck T, Brabletz S, Brabletz T. The EMT-activator ZEB1 promotes tumorigenicity by repressing stemness-inhibiting microRNAs. Nature Cell Biol. 2009; 11(12):1187–95.
8. Chitkara D, Mittal A, Mahato RI. miRNAs in pancreatic cancer: therapeutic potential, delivery challenges and strategies. Adv Drug Delivery Rev. 2014; 81C:34–52.
9. Li Y, VandenBoom TG II, Kong D, Wang Z, Ali S, Philip PA, Sarkar FH. Up-regulation of miR-200 and let-7 by natural agents leads to the reversal of epithelial-to-mesenchymal transition in gemcitabine-resistant pancreatic cancer cells. Cancer Res. 2009; 69:6704–6712. [PubMed: 19654291]
10. Singh S, Chitkara D, Kumar V, Behrman SW, Mahato RI. miRNA profiling in pancreatic cancer and restoration of chemosensitivity. Cancer Lett. 2013; 334:211–220. [PubMed: 23073476]

11. Johnson SM, Grosshans H, Shingara J, Byrom M, Jarvis R, Cheng A, Labourier E, Reinert KL, Brown D, Slack FJ. RAS is regulated by the let-7 microRNA family. Cell. 2005; 120:635–647. [PubMed: 15766527]
12. Trang P, Medina PP, Wiggins JF, Ruffino L, Kelnar K, Omotola M, Homer R, Brown D, Bader AG, Weidhaas JB, Slack FJ. Regression of murine lung tumors by the let-7 microRNA. Oncogene. 2010; 29:1580–1587. [PubMed: 19966857]
13. Patel K, Kollory A, Takashima A, Sarkar S, Faller DV, Ghosh SK. MicroRNA let-7 downregulates STAT3 phosphorylation in pancreatic cancer cells by increasing SOCS3 expression. Cancer Lett. 2014; 347:54–64. [PubMed: 24491408]
14. Sun TM, Du JZ, Yao YD, Mao CQ, Dou S, Huang SY, Zhang PZ, Leong KW, Song EW, Wang J. Simultaneous delivery of siRNA and paclitaxel via a “two-in-one” micelleplex promotes synergistic tumor suppression. ACS Nano. 2011; 5:1483–1494. [PubMed: 21204585]
15. Tsouris V, Joo MK, Kim SH, Kwon IC, Won YY. Nano carriers that enable co-delivery of chemotherapy and RNAi agents for treatment of drug-resistant cancers. Biotechnol Adv. 2014; 32:1037–50. [PubMed: 24924617]
16. Creixell M, Peppas NA. Co-delivery of siRNA and therapeutic agents using nanocarriers to overcome cancer resistance. Nano Today. 2012; 7:367–379. [PubMed: 26257819]
17. Mittal A, Chitkara D, Behrman SW, Mahato RI. Efficacy of gemcitabine conjugated and miRNA-205 complexed micelles for treatment of advanced pancreatic cancer. Biomaterials. 2014; 35:7077–7087. [PubMed: 24836307]
18. Danquah M, Fujiwara T, Mahato RI. Self-assembling methoxypoly(ethylene glycol)-*b*-poly(carbonate-*co*-L-lactide) block copolymers for drug delivery. Biomaterials. 2010; 31:2358–2370. [PubMed: 20018369]
19. Li F, Danquah M, Mahato RI. Synthesis and characterization of amphiphilic lipopolymers for micellar drug delivery. Biomacromolecules. 2010; 11:2610–2620. [PubMed: 20804201]
20. Kumar V, Mundra V, Mahato RI. Nanomedicines of Hedgehog inhibitor and PPAR-gamma agonist for treating liver fibrosis. Pharm Res. 2014; 31:1158–1169. [PubMed: 24249038]
21. Sezgin Z, Yuksel N, Baykara T. Preparation and characterization of polymeric micelles for solubilization of poorly soluble anticancer drugs. Eur J Pharm Biopharm. 2006; 64:261–268. [PubMed: 16884896]
22. Vorechovsky I, Benediktsson KP, Toftgard R. The patched/hedgehog/smoothened signalling pathway in human breast cancer: no evidence for H133Y SHH, PTCH and SMO mutations. Eur J Cancer. 1999; 35:711–713. [PubMed: 10505029]
23. Thiyagarajan S, Bhatia N, Reagan-Shaw S, Cozma D, Thomas-Tikhonenko A, Ahmad N, Spiegelman VS. Role of GLI2 transcription factor in growth and tumorigenicity of prostate cells. Cancer Res. 2007; 67:10642–10646. [PubMed: 18006803]
24. Mazumdar T, DeVecchio J, Shi T, Jones J, Agyeman A, Houghton JA. Hedgehog signaling drives cellular survival in human colon carcinoma cells. Cancer Res. 2011; 71:1092–1102. [PubMed: 21135115]
25. Ruiz i Altaba A, Stecca B, Sanchez P. Hedgehog—Gli signaling in brain tumors: stem cells and paradevelopmental programs in cancer. Cancer Lett. 2004; 204:145–157. [PubMed: 15013214]
26. Pasca di Magliano M, Sekine S, Ermilov A, Ferris J, Dlugosz AA, Hebrok M. Hedgehog/Ras interactions regulate early stages of pancreatic cancer. Genes Dev. 2006; 20:3161–3173. [PubMed: 17114586]
27. Proctor AE, Thompson LA, O’Bryant CL. Vismodegib: an inhibitor of the Hedgehog signaling pathway in the treatment of basal cell carcinoma. Ann Pharmacother. 2014; 48:99–106. [PubMed: 24259609]
28. Huang M, Tang SN, Upadhyay G, Marsh JL, Jackman CP, Shankar S, Srivastava RK. Embelin suppresses growth of human pancreatic cancer xenografts, and pancreatic cancer cells isolated from KrasG12D mice by inhibiting Akt and Sonic hedgehog pathways. PLoS One. 2014; 9:e92161. [PubMed: 24694877]
29. Wang Z, Li Y, Kong D, Banerjee S, Ahmad A, Azmi AS, Ali S, Abbruzzese JL, Gallick GE, Sarkar FH. Acquisition of epithelial–mesenchymal transition phenotype of gemcitabine-resistant

pancreatic cancer cells is linked with activation of the notch signaling pathway. Cancer Res. 2009; 69:2400–2407. [PubMed: 19276344]

30. Ahmad A, Maitah MY, Ginnebaugh KR, Li Y, Bao B, Gadgeel SM, Sarkar FH. Inhibition of Hedgehog signaling sensitizes NSCLC cells to standard therapies through modulation of EMT-regulating miRNAs. J Hematol Oncol. 2013; 6:77-8722-6-77. [PubMed: 24199791]
31. Torrisani J, Bournet B, du Rieu MC, Bouisson M, Souque A, Escourrou J, Buscail L, Cordelier P. let-7 MicroRNA transfer in pancreatic cancer-derived cells inhibits in vitro cell proliferation but fails to alter tumor progression. Hum Gene Ther. 2009; 20:831–844. [PubMed: 19323605]
32. Salmaso S, Caliceti P. Stealth properties to improve therapeutic efficacy of drug nanocarriers. J Drug Delivery. 2013; 2013:374252.
33. Fukushima S, Miyata K, Nishiyama N, Kanayama N, Yamasaki Y, Kataoka K. PEGylated polyplex micelles from triblock catiomers with spatially ordered layering of condensed pDNA and buffering units for enhanced intracellular gene delivery. J Am Chem Soc. 2005; 127:2810–2811. [PubMed: 15740090]
34. Kim HJ, Miyata K, Nomoto T, Zheng M, Kim A, Liu X, Cabral H, Christie RJ, Nishiyama N, Kataoka K. siRNA delivery from triblock copolymer micelles with spatially-ordered compartments of PEG shell, siRNA-loaded intermediate layer, and hydrophobic core. Biomaterials. 2014; 35:4548–4556. [PubMed: 24613051]
35. Lei J, Ma J, Ma Q, Li X, Liu H, Xu Q, Duan W, Sun Q, Xu J, Wu Z, Wu E. Hedgehog signaling regulates hypoxia induced epithelial to mesenchymal transition and invasion in pancreatic cancer cells via a ligand-independent manner. Mol Cancer. 2013; 12:66-4598-12-66. [PubMed: 23786654]
36. Thayer SP, di Magliano MP, Heiser PW, Nielsen CM, Roberts DJ, Lauwers GY, Qi YP, Gysin S, Fernandez-del Castillo C, Yajnik V, Antoniu B, McMahon M, Warshaw AL, Hebrok M. Hedgehog is an early and late mediator of pancreatic cancer tumorigenesis. Nature. 2003; 425:851–856. [PubMed: 14520413]
37. Morton JP, Mongeau ME, Klimstra DS, Morris JP, Lee YC, Kawaguchi Y, Wright CV, Hebrok M, Lewis BC. Sonic hedgehog acts at multiple stages during pancreatic tumorigenesis. Proc Natl Acad Sci U S A. 2007; 104:5103–5108. [PubMed: 17372229]
38. Kim EJ, Sahai V, Abel EV, Griffith KA, Greenson JK, Takebe N, Khan GN, Blau JL, Balis UG, Craig R, Zalupski MM, Simeone DM. Pilot Clinical Trial of Hedgehog Pathway Inhibitor GDC-0449 (Vismodegib) in Combination with Gemcitabine in Patients with Metastatic Pancreatic Adenocarcinoma. Clin Cancer Res. 2014; 20:5937–5945. [PubMed: 25278454]
39. Lee JJ, Perera RM, Wang H, Wu DC, Liu XS, Han S, Fitamant J, Jones PD, Ghanta KS, Kawano S, Nagle JM, Deshpande V, Boucher Y, Kato T, Chen JK, Willmann JK, Bardeesy N, Beachy PA. Stromal response to Hedgehog signaling restrains pancreatic cancer progression. Proc Natl Acad Sci U S A. 2014; 111:E3091–E4100. [PubMed: 25024225]
40. Rhim AD, Oberstein PE, Thomas DH, Mirek ET, Palermo CF, Sastra SA, Dekleva EN, Saunders T, Becerra CP, Tattersall IW, Westphalen CB, Kitajewski J, Fernandez-Barrena MG, Fernandez-Zapico ME, Iacobuzio-Donahue C, Olive KP, Stanger BZ. Stromal elements act to restrain, rather than support, pancreatic ductal adenocarcinoma. Cancer Cell. 2014; 25:735–747. [PubMed: 24856585]
41. Mathew E, Zhang Y, Holtz AM, Kane KT, Song JY, Allen BL, di Magliano MP. Dosage-Dependent Regulation of Pancreatic Cancer Growth and Angiogenesis by Hedgehog Signaling. Cell Rep. 2014; 9:484–494. [PubMed: 25310976]
42. De Jesus-Acosta A, O'Dwyer PJ, Ramanathan RK, Von Hoff DD, Maitra A, Rasheed Z, et al. A phase II study of vismodegib, a hedgehog (Hh) pathway inhibitor, combined with gemcitabine and nab-paclitaxel (nab-P) in patients (pts) with untreated metastatic pancreatic ductal adenocarcinoma (PDA). J Clin Oncol. 2014; 32(Suppl 3) Abstract 257.

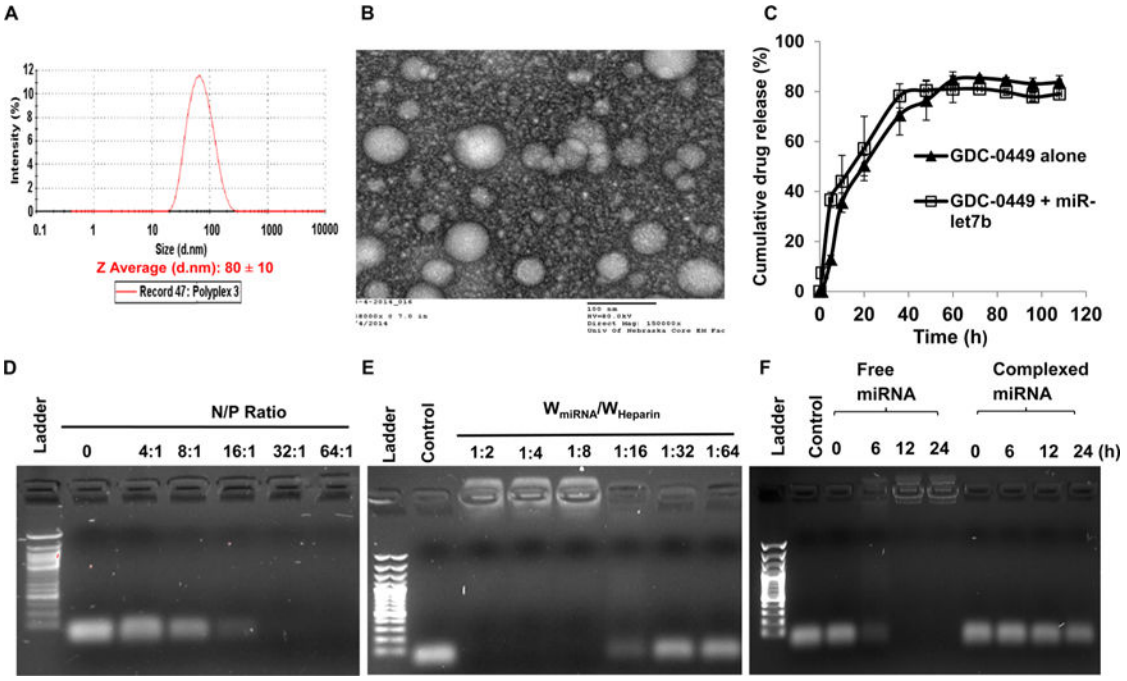

Figure 1.

Micelle preparation and characterization. (A) Particle size distribution of miR-let7b complexed and GDC-0449 encapsulated micelles using dynamic light scattering. (B) Micelle morphology determined by transmission electron microscope (TEM). (C) GDC-0449 release profile from micelles with or without miRNA, (D) complex formation ability of micelles to miRNA at different N/P ratios, (E) miRNA dissociation from micelles by heparin, and (F) miRNA stability in the presence of 25% FBS. Equal amount of each sample was incubated with 10 μL of FBS at 37 °C for 0, 6, 12, and 24 h prior to gel electrophoresis.

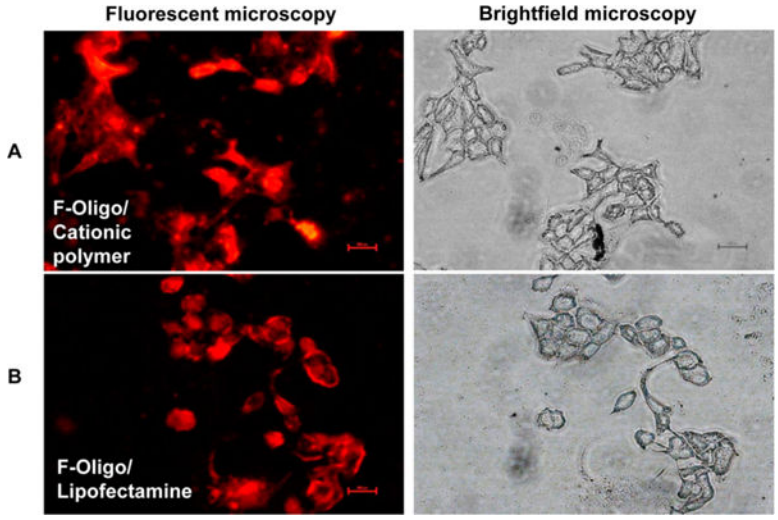

Figure 2.

Transfection efficiency of fluorescent labeled Block-IT oligo loaded micelles into Capan-1 cells. (A) Oligo complexed micelles and (B) oligo/lipofectamine complexes. Right panesl are optical images of cells (DIC). After 3 h post-transfection, cells were washed, fixed, and mounted for microscopy.

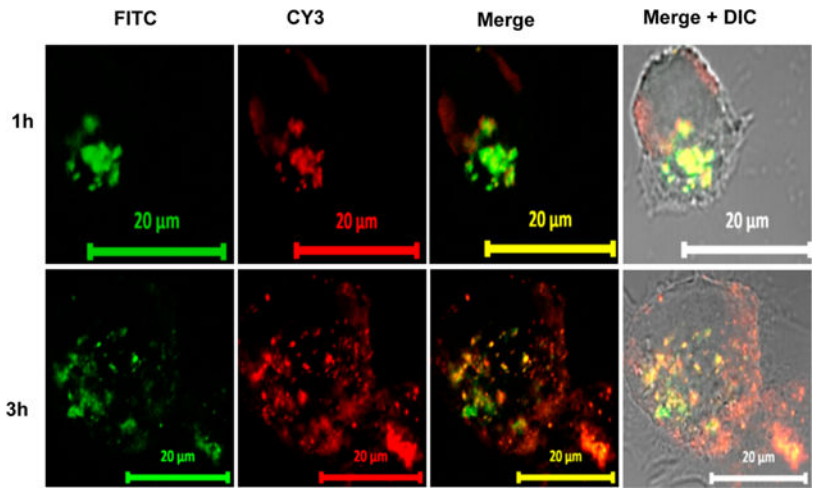

Figure 3.

Confocal microscopy of MIA-PaCa-2 cells exposed to CY3-oligo complexed micelles. Cells were exposed to micelles for 1–3 h. Fluorescence of the micellar core (red) and shell of the endosomes (green) is highly colocalized, as indicated by the yellow signal in the merged images. Scale bar: 20 μm.

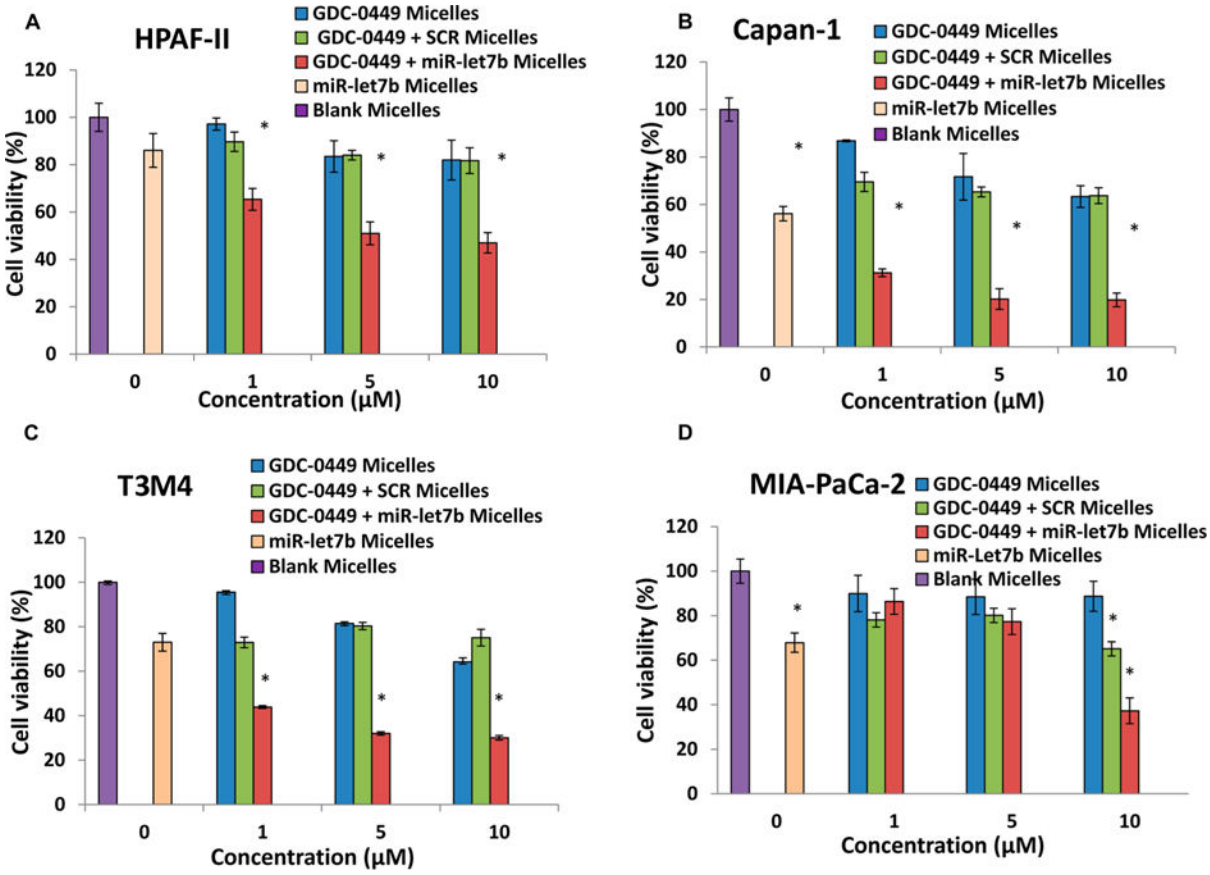

Figure 4.

Effect of GDC-0449 and miR-let7b on cell viability in human pancreatic cancer cell line by micelles. (A) HPAF-II, (B) Capan-1, (C) T3M4 and (D) MIA PaCa-2 cells (5000/well) were treated with micelles containing (blue bars) GDC-0449 (0, 1, 5, and 10 μM), (green bars) GDC-0449 and scrambled miRNA, (red bars) GDC-0449 and miR-let7b (10 pmol), (peach bars) miR-let7b alone, and (purple bars) blank for 48 h. Cell viability was measured by MTT assay at the end of incubation period. Data represent the mean ± SD (n = 3).

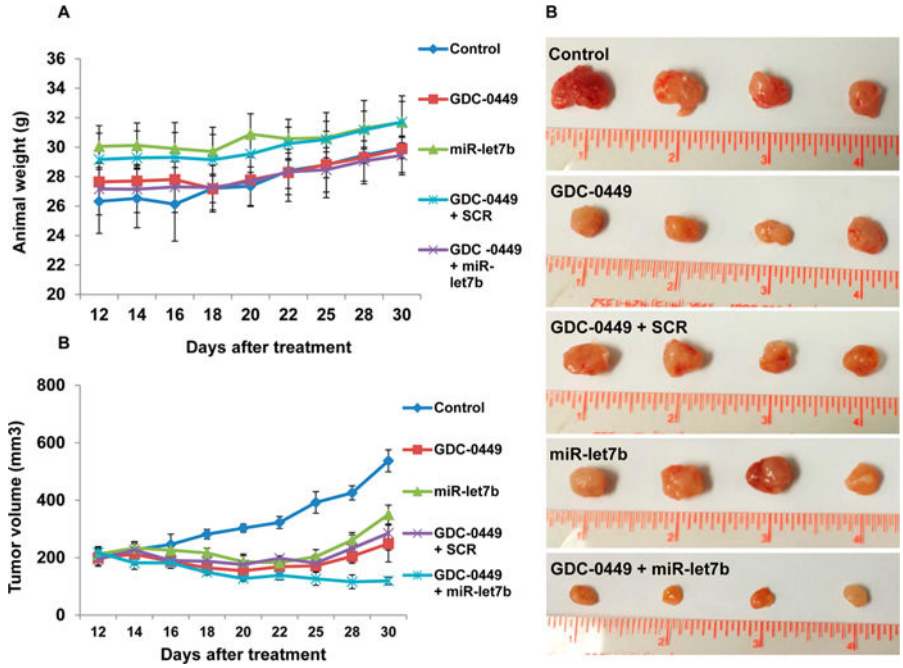

Figure 5.

In vivo efficacy of mPEG-*b*-PCC-*g*-DC-*g*-TEPA micelles carrying GDC-0449 and miR-let7b in tumor bearing mice. Tumors were developed by subcutaneous injection of (3×10^6) of MIA PaCa-2 cells in the left flank of athymic nude mice. When the tumor size reached 200 mm^3, mice were injected intratumorally with one of the following formulations: blank micelles, micelles carrying GDC-0449, micelles carrying GDC-0449 and scrambled miRNA, and micelles carrying GDC-0449 and miR-let7b. Dose was 10 mg/kg GDC-0449 and 2 mg/kg miR-let7b or scrambled miRNA. (A) Animals body weight during treatment, (B) tumor volume, and (C) representative tumor size of various treatment groups. GDC-0449/miR-let7b micelles decreased the rate of tumor growth compared to monotherapy. Data expressed as the mean ± SE ($n = 5$).

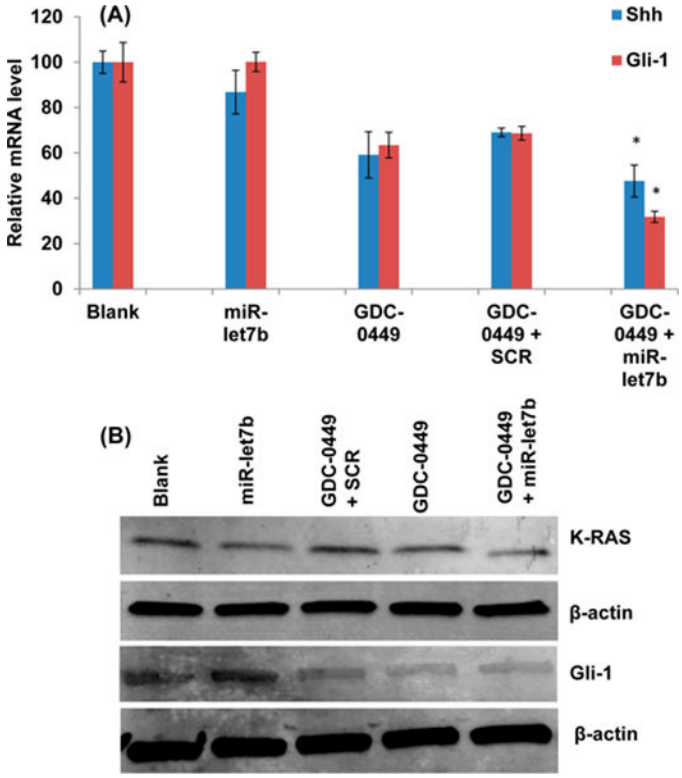

Figure 6.

RT-PCR and Western blot of tumor samples. (A) GDC-0449/miR-let7b treated animals showed downregulated relative mRNA levels of Shh and Gli compared to control animals ($n = 3$, $p < 0.05$). (B) Western blot of Gli-1 and K-RAS.

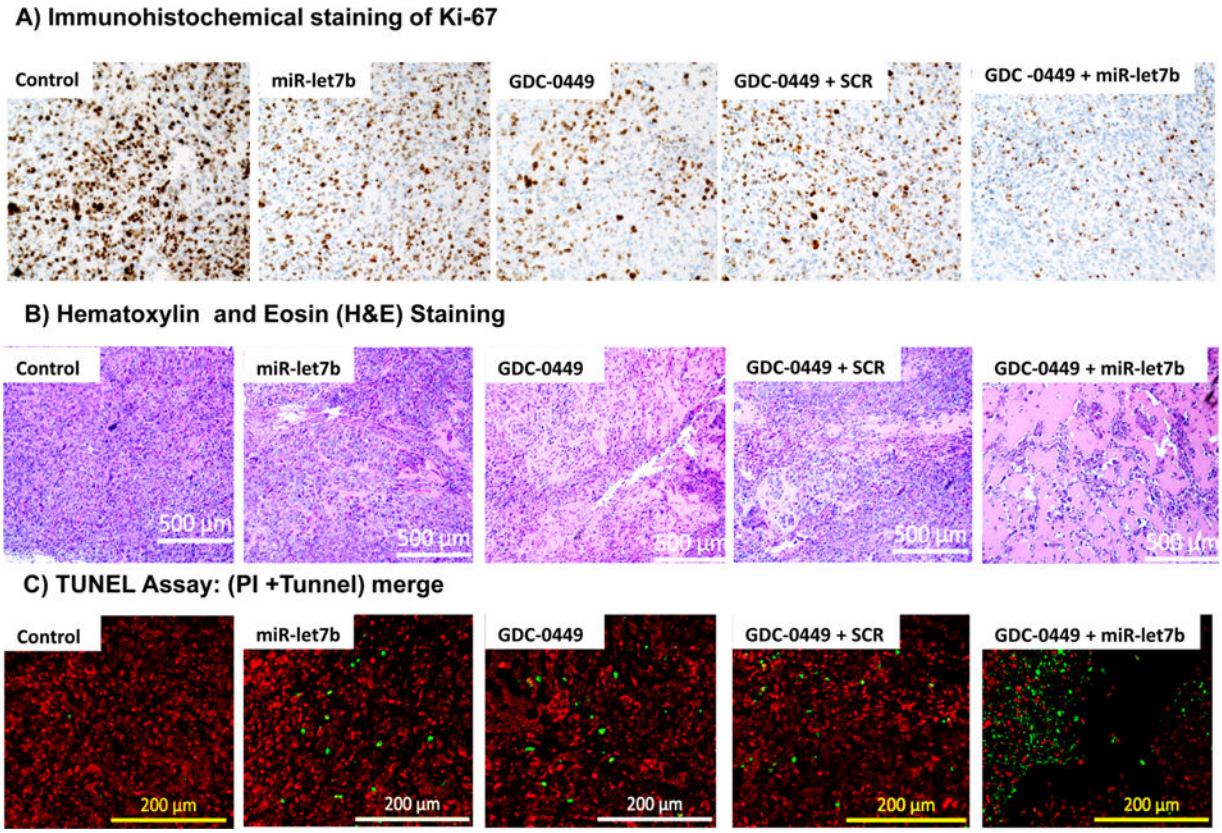

Figure 7.

Analysis of tumor samples for Ki-67 staining, hematoxylin and eosin (H&E) staining, and (C) TUNEL assay for apoptosis. (A) Immunohistochemical staining of Ki-67, (B) H&E staining of peripheral tumor regions, and (C) apoptosis in tumor cells as indicated by the green fluorescence of TUNEL, while red spots mark the cells with propidium iodide (PI) staining.